Grid-Free MIMO Beam Alignment through Site-Specific Deep Learning

Yuqiang Heng, and Jeffrey G. Andrews, *Fellow, IEEE*

Abstract

Beam alignment is a critical bottleneck in millimeter wave (mmWave) communication. An ideal beam alignment technique should achieve high beamforming (BF) gain with low latency, scale well to systems with higher carrier frequencies, larger antenna arrays and multiple user equipments (UEs), and not require hard-to-obtain context information (CI). These qualities are collectively lacking in existing methods. We depart from the conventional codebook-based (CB) approach where the optimal beam is chosen from quantized codebooks and instead propose a grid-free (GF) beam alignment method that directly synthesizes the transmit (Tx) and receive (Rx) beams from the continuous search space using measurements from a few site-specific probing beams that are found via a deep learning (DL) pipeline. In realistic settings, the proposed method achieves a far superior signal-to-noise ratio (SNR)-latency trade-off compared to the CB baselines: it aligns near-optimal beams 100x faster or equivalently finds beams with 10-15 dB better average SNR in the same number of searches, relative to an exhaustive search over a conventional codebook.

Index Terms

5G mobile communication, Beam management, Deep learning, Millimeter wave communication.

I. Introduction

MmWave devices require highly directional BF to compensate for the severe isotropic path loss and to achieve viable signal strength. To reduce the cost and power consumption of a fully digital system, practical mmWave systems often adopt analog beams that concentrate energy in a small angular area. On the other hand, these narrow beams are susceptible to changes in the propagation environment such as blockage and reflection. It is critical for mmWave base stations

Yuqiang Heng and Jeffrey G. Andrews are with 6G@UT, the Wireless Networking and Communications Group (WNCG), the University of Texas at Austin, Austin, TX 78701 USA. Email: (yuqiang.heng@utexas.edu, jandrews@ece.utexas.edu). A preliminary version of this work will appear in Globecom 2022 [1]. Date of current version: September 20, 2022.

(BSs) and UEs to find good BF directions during initial connection and then track these analog beams as the propagation conditions change, such as when a UE moves and rotates. As future cellular systems move to unlock larger bandwidths at higher carrier frequencies extending to the so-called "Terahertz" bands of up to 300 GHz, devices will adopt ever denser antenna arrays and narrower beams. As a result, beam management – the process of discovering and maintaining good analog BF directions – is a critical bottleneck that will only worsen as we move towards 6G and beyond.

A. Background and related work

Existing beam management approaches typically assume a "grid-of-beams" or CB framework, where BSs and UEs adopt codebooks of quantized BF angles. In order to ensure coverage in any site, the quantized beams usually distribute energy uniformly in the angular space, such as by using discrete Fourier transform (DFT) codebooks. In this context, the problem of beam alignment becomes selecting the optimal beams from the finite codebooks at the BS and the UE. The most widely adopted method of beam selection is through a search. For instance, 5G NR adopts a beam management framework based on beam sweeping, measurement and reporting [2], [3]. In the downlink, the BS exhaustively searches its codebook by periodically sending beamformed reference signals (RSs) called Synchronization Signal Blocks (SSBs). The UE measures and reports the received signal strength. And the BS selects the best beam based on the UE's feedback. The obvious drawback of an exhaustive search is its beam sweeping latency, which grows linearly with the total number of beam pairs. As systems move up the spectrum and adopt narrower beams, the size of the codebook increases accordingly. A Terahertz system may easily adopt tens of thousands of beam pairs, rendering the the exhaustive search infeasible due to the prohibitive beam sweeping latency. A hierarchical search can reduce the latency for a single UE. By sweeping wider beams first and progress to narrower child beams, it iteratively reduces the search space. In the 5G NR framework, the BS can use SSBs to sweep the wide beams and use the more flexible Channel State Information Reference Signals (CSI-RSs) for narrow-beam refinement. On the other hand, the radiation patterns of the wide beams need to be carefully designed since the hierarchical search is more prone to search errors caused by noisy measurements and imperfect wide-beam shapes [4], [5].

Another way to reduce the beam sweeping latency is to leverage context information (CI). The optimal beam pair of a link is intuitively a function of the topology of the propagation

environment and the locations of the BS and the UE. Such spatial properties can be captured through CI such as sub-6 GHz out-of-band (OOB) measurements [6], global navigation satellite system (GNSS) coordinates of the UE [7], [8], radar measurements [9], [10], images captured by cameras and 3D point clouds of the environment [11], [12]. By constructing a mapping from the CI to the index of the optimal beam through a lookup table or machine learning (ML) models, the search space can be substantially reduced. However, these CI-based methods are difficult to be standardized and widely-adopted in practice due to the requirement of additional sensors and the varying hardware capabilities of mmWave devices. They are also not suitable for standalone systems due to the need of a robust feedback link usually occupying a lower frequency band.

B. Site-specific adaptation

A promising way to reduce the beam sweeping latency is by site-specific adaptation. In scenarios where the angle-of-arrival (AoA) and angle-of-departure (AoD) distributions are highly non-uniform, such as in particular environment topologies and when there are several spatial clusters of UEs, some beams in a uniform codebook may never get used. Leveraging this fact, the BS can compute the statistics of the entire codebook after an exhaustive training phase and prioritize the most frequently used beams [13], [14]. By training using explicit Channel State Information (CSI) [15] or through implicit rewards in a reinforcement learning (RL) framework [16], neural networks (NNs) can generate smaller codebooks from scratch that adapt to the environment and strategically direct energy towards the UEs. The data-driven approach can also help select analog beams from standard codebooks using sensing measurements by optimizing the mapping function [17] or jointly learning the sensing beams and the mapping function [18].

Compared to CB beam management methods whose BF gain is limited by the resolution of the codebook, a GF approach extends the search space for the optimal beam to the high-dimensional continuous space and can in theory achieve better gain. For instance, maximum ratio transmission (MRT) is known to be optimal under the unit power constraint and equal ratio transmission (EGT) under the unit modulus constraint. However, they require full CSI to compute the BF weights, which is generally unavailable before beam alignment. Furthermore, even with CSI, finding the optimal EGT and equal ratio combining (EGC) beams requires a grid search over possible weights in the multiple-input multiple-output (MIMO) setting and is computationally prohibitive [19]. Recent works have explored directly predicting the hybrid BF

weights for the BS without full CSI by learning sensing matrices [20] or a sequence of interactive sensing vectors based on feedback of previous measurements [21].

In our previous work [22], we proposed a CB beam alignment method that uses the measurements of a few site-specific probing beams to predict the index of the optimal Tx narrow beam. However, it benefits significantly from trying a few candidate beams for each UE. As a result, the gain in the beam sweeping overhead diminishes with increasing number of UEs. This is a common and important limitation of many existing methods: the hierarchical search requires searching all child beams, many CI-based models require trying the most likely candidates, and active learning-based methods require sweeping a different sequence of sensing beams for each UE. A beam sweeping procedure needs to be repeated for all UEs in the cell, each of which may require a different set of beams. Hence the total beam sweeping latency increases linearly with the number of UEs, which can be large and unknown in cellular systems. In CB approaches, eventually the entire codebook will need to be searched, a major shortcoming of many of the aforementioned methods.

C. Contributions

In this work, we propose DL-GF, an one-shot grid-free (GF) beam alignment method based on unsupervised deep learning (DL). The proposed method learns a small number of probing beams through site-specific training and directly predicts the optimal analog BF vectors without using a quantized codebook. It possesses several qualities of an ideal beam alignment method, many of which are lacking in existing approaches:

- **High BF gain beyond standard codebooks.** The proposed method synthesizes the analog beams from the continuous search space instead of selecting from a quantized codebook. With the additional degree of freedom, the synthesized beams can achieve better BF gain compared to choosing optimally from large quantized codebooks.
- **Low beam sweeping latency with optimal scaling.** With site-specific training, the proposed method requires just sweeping a few probing beam pairs to capture sufficient channel information. Unlike many existing approaches that require sweeping a few candidate beams or child beams for each UE, the proposed method synthesizes the analog beams in one-shot. As a result, the beam sweeping latency does not increase with the number of UEs. In our setting, DL-GF reduces the beam sweeping overhead by over 500× vs. the exhaustive CB method regardless of the number of UEs.

- **Easy to adopt in cellular standards.** The proposed method does not require hard-to-obtain CI such as the location of UEs and OOB measurements. Instead, it purely relies on measuring and reporting a few probing beams. The probing beams are also optimized for coverage, allowing the BS to discover new UEs.
- **Joint Tx-Rx beam alignment.** Unlike many existing methods that only consider beam alignment for the BS, the proposed method synthesizes the analog beam for both the BS and the UE. It does not require an additional beam alignment process for the UE. The synthesized Tx and Rx beam pairs are jointly optimized to achieve high BF gain, even when the UEs have random orientations.

The rest of this article is organized as follows. The system model is described in Section II. The proposed beam alignment approach, the appropriate metrics and the baselines of comparison are explained in Section III. The datasets used are described in Section IV. The simulation results are presented in Section V. Finally, we provide the conclusion and final remarks in Section VI.

Notation: The following notations are used in this paper: $|a|$ denotes the magnitude of the scalar a, $||\mathbf{A}||_{\mathrm{F}}$ denotes the Frobenius norm, $\mathbf{A}^{\mathrm{real}}, \mathbf{A}^{\mathrm{imag}}$ denote the real and imaginary parts of a complex matrix $\mathbf{A}$, $\mathbf{A}^T$ denotes the transpose, $\mathbf{A}^H$ denotes the conjugate transpose, $[\mathbf{a}]_i$ denotes the ith element of the vector $\mathbf{a}$, $\mathbf{a} \otimes \mathbf{b}$ denotes the Kronecker product, $\mathbf{A} \oslash \mathbf{B}$ denotes the element-wise division and $\mathbf{A}^{|\cdot|}$ denotes the element-wise magnitude.

II. System Model

A MIMO system is considered where the BS has an array of N_{T} antennas. the UE has an array of N_{R} antennas and both perform beam alignment. A geometric channel model with L paths is adopted:

$$\mathbf{H} = \sum_{l=1}^{L} \alpha_l e^{j(\theta_l - 2\pi\tau_l B)} \mathbf{a}_{\mathrm{R}}(\omega_l^{az}, \omega_l^{el}) \mathbf{a}_{\mathrm{T}}(\phi_l^{az}, \phi_l^{el})^H, \tag{1}$$

where $\mathbf{a}_{\mathrm{T}}, \mathbf{a}_{\mathrm{R}}$ are the Tx and Rx array response vectors, $\alpha_l, \theta_l, \tau_l$ are the gain, Doppler shift and delay, $\omega_l^{az}, \omega_l^{el}, \phi_l^{az}, \phi_l^{el}$ are the azimuth and elevation AoA and AoD of path l. For a uniform planar array (UPA) with N_y and N_z antennas in the $y-z$ plane, its array response vector is given by:

$$\mathbf{a}(\phi^{az}, \phi^{el}) = \mathbf{a}_z(\phi^{el}) \otimes \mathbf{a}_y(\phi^{az}, \phi^{el}), \tag{2}$$

where

$$\mathbf{a}_y(\phi^{az}, \phi^{el}) = \begin{bmatrix} 1 & e^{j\frac{2\pi}{\lambda}d\sin\phi^{az}\sin\phi^{el}} & \dots & e^{j(N_y-1)\frac{2\pi}{\lambda}d\sin\phi^{az}\sin\phi^{el}} \end{bmatrix}^T, \tag{3}$$

$$\mathbf{a}_z(\phi^{el}) = \begin{bmatrix} 1 & e^{j\frac{2\pi}{\lambda}d\cos\phi^{el}} & \dots & e^{j(N_z-1)\frac{2\pi}{\lambda}d\cos\phi^{el}} \end{bmatrix}^T, \tag{4}$$

λ is the carrier wavelength and d is the antenna spacing.

In the downlink, if the BS adopts a Tx beam $\mathbf{f} \in \mathbb{C}^{N_\mathrm{T}\times 1}$ and transmit a symbol s and the UE adopts a Rx beam $\mathbf{w} \in \mathbb{C}^{N_\mathrm{R}\times 1}$, the received signal can be written as

$$y = \sqrt{P_\mathrm{T}}\mathbf{w}^H\mathbf{H}\mathbf{f}s + \mathbf{w}^H\mathbf{n}, \tag{5}$$

where P_T is the Tx power and $\mathbf{n} \sim \mathcal{CN}(0, \sigma^2\mathbb{I})$ is a complex additive white Gaussian noise (AWGN). Assuming unit-power transmitted symbols, the SNR achieved by the beam pair is

$$\mathrm{SNR} = \frac{P_\mathrm{T}|\mathbf{w}^H\mathbf{H}\mathbf{f}|^2}{|\mathbf{w}^H\mathbf{n}|^2}. \tag{6}$$

The BS and the UEs are assumed to perform analog BF only. Each device has a single radio frequency (RF) chain connected to an array of phase shifters. Hence the BF vectors satisfy the unit-power, constant modulus constraint:

$$|[\mathbf{f}]_i| = \frac{1}{\sqrt{N_\mathrm{T}}}, i = 1, \dots, N_\mathrm{T} \tag{7}$$

$$|[\mathbf{w}]_j| = \frac{1}{\sqrt{N_\mathrm{R}}}, j = 1, \dots, N_\mathrm{R}. \tag{8}$$

In systems that adopts hybrid BF, the BS and the UE may first undergo beam alignment and select good analog beams, then perform digital precoding over the effective channel. The joint optimization of analog and digital BF is left for future work.

The orientation of a UE is modeled with random rotations with respect to the local coordinate system which is attached to and rotates with the UE [23]. Each UE first rotates by the z axis, then by the new y axis, and finally by the new x axis. The angles of the three elemental rotations are modeled as random variables. The AoA of the channel is then adjusted according to the orientation of the UE. A more sophisticated model may consider the shape of the UE and self–blockage of the device, which is left for future work.

III. The Proposed Method, Metrics and Baselines

Our objective is to directly predict optimal Tx and Rx beams without searching large codebooks or candidate beams. In our previous work [22], we demonstrated that a NN classifier can accurately select the optimal beam index from a large codebook using measurements of a few learned site-specific probing beams, i.e., each BS learns unique probing beams that are well-suited to its propagation environment. Inspired by this idea, we propose to learn a small number of probing beams at both the BS and the UE and use their measurements to synthesize the optimal narrow beam pair from the continuous search space. The BS first sweeps $N_{\mathbf{F}}$ Tx probing beams while the UE measures the received signal power using $N_{\mathbf{W}}$ Rx probing beams. After the probing-beam sweeping phase, the UE uses the collected measurements as inputs to its beam synthesizer function f_{R} to generate its Rx beam. The measurements are also fed back to the BS, which uses them as inputs to its own beam synthesizer function f_{T} to generate the Tx beam.

Let $\mathbf{F} \in \mathbb{C}^{N_{\mathrm{T}} \times N_{\mathbf{F}}}, \mathbf{W} \in \mathbb{C}^{N_{\mathrm{R}} \times N_{\mathbf{W}}}$ be matrices representing the BS and UE probing beams. The composite received signal $\mathbf{Y} \in \mathbb{C}^{N_{\mathbf{W}} \times N_{\mathbf{F}}}$ consisting of the received signal of all combinations of probing beams can be written as

$$\mathbf{Y} = \sqrt{P_T}\mathbf{W}^H\mathbf{H}\mathbf{F}\mathbf{s} + \mathbf{W}^H\mathbf{n}, \tag{9}$$

where $\mathbf{s}$ is the vector of transmitted signals and $\mathbf{n} \sim \mathcal{CN}(0, \sigma^2\mathbb{I})$ is the measurement noise.

We focus on the special case where $N_{\mathbf{F}} = N_{\mathbf{W}} = N_{\text{probe}}$: the BS sweeps N_{probe} probing beams while the UE uses a different Rx beam for each Tx probing beam so that the total number of probing beam pairs is N_{probe}. The UE then reports the N_{probe} received signal power measurements. As a result, the input feature to the beam synthesizer functions is

$$\mathbf{z} = \left[|[\mathrm{diag}(\mathbf{Y})]_1|^2 \quad \cdots \quad |[\mathrm{diag}(\mathbf{Y})]_{N_{\text{probe}}}|^2 \right]^T. \tag{10}$$

In principle, both the measurement and the feedback procedures are flexible and can be design choices. For example, the number of Tx and Rx probing beams can be arbitrary. The UE can measure and feedback any or all combinations of probing beams, and the beam synthesizer functions can utilize the full $\mathbb{C}^{N_{\mathbf{W}} \times N_{\mathbf{F}}}$ measurement matrix to generate the BF vectors. The UE may also feedback just $N_{\mathbf{F}}$ measurements corresponding to the strongest Rx probing beam for each Tx probing beam. The specific design considered in this work is motivated by our wish to

reduce the measurement and feedback overhead, i.e., $N_{\text{probe}} \ll N_{\mathbf{F}} N_{\mathbf{W}}$. Furthermore, it is also more compatible with the RS feedback procedure in 5G NR, where the UE beam is transparent to the BS. However, there is extensive scope for future work exploring other approaches.

A. Problem formulation

The parameters of the proposed method include the Tx and Rx probing beams $\mathbf{F}, \mathbf{W}$ as well as the beam synthesizers $f_{\text{T}}, f_{\text{R}}$, which need to be optimized with respect to a utility function. With the unit modulus constraint of the probing and predicted beams in mind, the optimization problem can be written as:

$$
\begin{aligned}
\max_{\mathbf{F},\mathbf{W},f_{\text{T}},f_{\text{R}}} \quad & \mathcal{U} \\
\text{s.t.} \quad \mathbf{v}_{\text{T}} &= f_{\text{T}}(\mathbf{z}) \\
\mathbf{v}_{\text{R}} &= f_{\text{R}}(\mathbf{z}) \\
|[\mathbf{v}_{\text{T}}]_i| &= \tfrac{1}{\sqrt{N_{\text{T}}}}, \quad \forall i = 1, \cdots, N_{\text{T}} \\
|[\mathbf{v}_{\text{R}}]_i| &= \tfrac{1}{\sqrt{N_{\text{R}}}}, \quad \forall i = 1, \cdots, N_{\text{R}} \\
|[\mathbf{F}]_{i,j}| &= \tfrac{1}{\sqrt{N_{\text{T}}}}, \quad \forall i = 1, \cdots, N_{\text{T}}, \quad \forall j = 1, \cdots, N_{\mathbf{F}} \\
|[\mathbf{W}]_{i,j}| &= \tfrac{1}{\sqrt{N_{\text{R}}}}, \quad \forall i = 1, \cdots, N_{\text{R}}, \quad \forall j = 1, \cdots, N_{\mathbf{W}}.
\end{aligned}
\tag{11}
$$

There are several considerations when designing the utility function. The beam synthesizer functions should generate beams that tend to maximize the BF gain for each channel realization. The probing beams in $\mathbf{F}$ and $\mathbf{W}$ serve two important purposes. First, they provide helpful information to the beam synthesizers and thus should capture characteristics of the channel. Second, they should allow the BS to discover new UEs during the initial access (IA) process and thus should satisfy a minimum SNR requirement. Since the optimal BF vectors can be easily computed in closed-form in the simpler multiple-input single-output (MISO) or single-input multiple-output (SIMO) setting, the synthesized beams can be optimized to resemble the optimal EGT or EGC beams by minimizing a supervised loss function such as the mean square error (MSE) in [15]. However, finding the EGT and EGC beam pairs in the MIMO setting requires solving its own non-convex optimization problem and may require a grid-search over possible weights, making a supervised utility function undesirable. To this end, we propose a two-component unsupervised utility function that does not require explicit labels for the probing or synthesized beams:

$$\mathcal{U} = \begin{cases} \mathcal{U}_{\mathrm{BF}} & \text{if } \mathcal{H}_{\mathrm{IA}} = \mathcal{H} \\ \gamma \mathcal{U}_{\mathrm{BF}} + (1-\gamma)\mathcal{U}_{\mathrm{IA}} & \text{otherwise} \end{cases} \tag{12}$$

$$\mathcal{U}_{\mathrm{BF}} = \mathop{\mathbb{E}}_{\mathbf{H}\in\mathcal{H}} \left[\frac{|\mathbf{v}_{\mathrm{R}}^H \mathbf{H} \mathbf{v}_{\mathrm{T}}|^2}{||\mathbf{H}||_{\mathrm{F}}^2} \right] \tag{13}$$

$$\mathcal{U}_{\mathrm{IA}} = \mathop{\mathbb{E}}_{\mathbf{H}\in\mathcal{H}\setminus\mathcal{H}_{\mathrm{IA}}} \left[\max_{\mathbf{f}\in\mathcal{F},\mathbf{w}\in\mathcal{W}} \frac{|\mathbf{w}^H \mathbf{H} \mathbf{f}|^2}{||\mathbf{H}||_{\mathrm{F}}^2} \right] \tag{14}$$

$$\mathcal{H}_{\mathrm{IA}} = \{\mathbf{H} \in \mathcal{H} : \max_{\mathbf{f}\in\mathcal{F},\mathbf{w}\in\mathcal{W}} \frac{P_T |\mathbf{w}^H \mathbf{H} \mathbf{f}|^2}{|\mathbf{w}^H \mathbf{n}|^2} \geq \mathrm{SNR}_{\mathrm{TH}}\} \tag{15}$$

Let $\mathcal{H}$ denote the set of channel realizations corresponding to possible UE locations in the cell. The set of Tx and Rx probing beams are denoted by $\mathcal{F}$ and $\mathcal{W}$. The first term $\mathcal{U}_{\mathrm{BF}}$ focuses on the BF gain of the synthesized beams and is the end-to-end objective. An obvious choice for the utility function is the average SNR or achievable rate of the predicted beam pairs, such as adopted in [20]. However, it tends to emphasize UEs with good channels more and neglect cell edge UEs. In order to provide better coverage to all UEs, we maximize the average BF gain normalized by the channel norm to give equal emphasis even for UEs with worse channels. The second term $\mathcal{U}_{\mathrm{IA}}$ ensures the coverage of the probing beams. It maximizes the average normalized BF gain of the strongest probing beam pairs for those UEs that cannot meet the minimum SNR threshold $\mathrm{SNR}_{\mathrm{TH}}$ with any of the probing beam pairs. The coefficient $\gamma \in [0, 1]$ is a design parameter to balance the trade-off between the gain of the synthesized beams and of the probing beams.

B. The proposed NN architecture

The optimization problem in 11 is difficult to solve since the unit-modulus constraints are non-convex while the functions f_{T} and f_{R} are generally unknown. We propose to parameterize the probing beams $\mathbf{F}, \mathbf{W}$ as well as the beam synthesizers $f_{\mathrm{T}}, f_{\mathrm{R}}$ using NNs and optimize them in a data-driven fashion. The overall NN architecture is illustrated in Fig. 1. During the offline training phase, the input to the entire NN model are the channel matrices. The Tx and Rx probing beams are implemented in the complex NN module as two complex matrices. The entire complex NN module can be considered to perform an affine transformation of the channel matrix. To enforce the unit-modulus constraint, the complex matrices are normalized element-wise by the absolute

value. We find this implementation to perform better empirically compared to the implementation used in our previous work [22], where the complex matrices are computed using the phase-shift values. The complex NN module computes the composite matrix of received signals of all combinations of probing beams in 9. The power of the N_{probe} probing beam pairs corresponding to the diagonal elements are extracted and fed into the Tx and Rx beam synthesizer functions, each parameterized using an multilayer perceptron (MLP). The MLP consists of 2 hidden layers with rectified linear unit (ReLU) activation and a final linear layer outputting the real and imaginary parts of the synthesized BF vector. The final predicted beams are normalized element-wise to enforce the unit-modulus constraint. With each batch of training channel realizations, the utility can be computed using the BF gain of the synthesized beams and that of the best probing beam pairs. The Tx and Rx probing beams as well as the beam synthesizer functions are trained through stochastic gradient descent and backpropagation.

C. Practicality of the proposed method

The NN model is trained offline prior to deployment. The training data can be obtained through ray-tracing simulations or from measurements. Due to the difficulty of obtaining CSI in real time, online training and adaptation of the NN remain an open research problem. On the other hand, the model proves to be fairly robust against imperfect training data, as we will show in Section V-C2. After the offline training phase, the probing beam pairs are extracted from the complex NN module and implemented in RF. The beam synthesizers $f_{\text{T}}, f_{\text{R}}$ are implemented at the BS and the UE respectively. During deployment, the BS and the UE periodically sweep the probing beam pairs while the UE measures the received signal power. The probing measurements are then reported to the BS. The BS and the UE use the probing measurements as inputs to f_{T} and f_{R} to synthesize the Tx and Rx beams. Since the probing beams and the beam synthesizers are site-specific, $\mathbf{W}$ and f_{R} need to be transmitted to the UEs. In a non-standalone system, this can be done through a lower-frequency side link. A new UE can then complete IA using the strongest probing beam pair. We have previously shown that the Tx probing beams can be used for IA in the MISO setting [1]. Therefore in a standalone system, the BS may sweep the Tx probing beams while a new UE receives using a quasi-omnidirectional beam. The UE can complete IA with the strongest Tx probing beam, download the Rx components $\mathbf{W}$ and f_{R}, then perform the full joint Tx-Rx beam alignment.

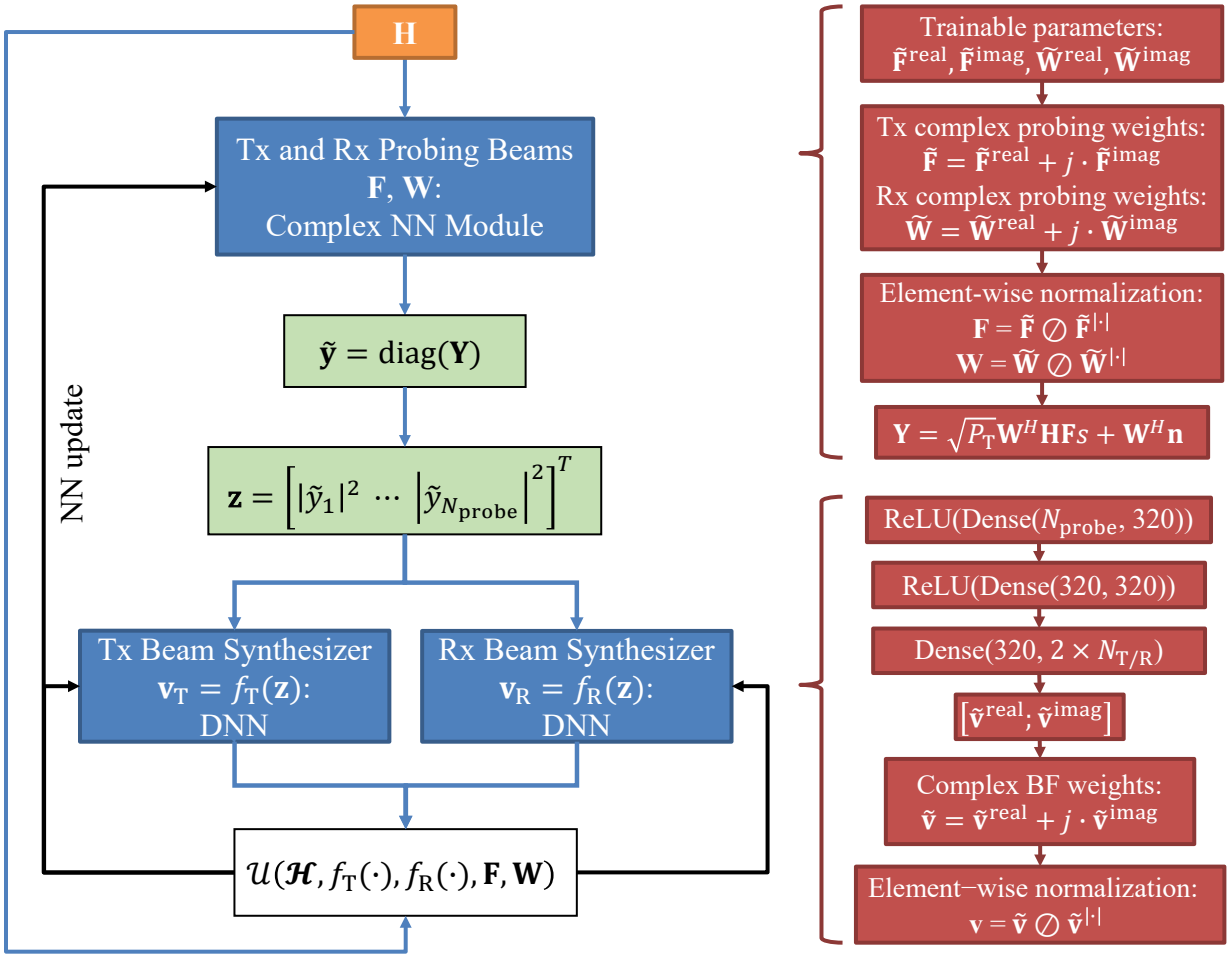

Fig. 1: The architecture of the proposed NN, including the probing beam pairs $\mathbf{F}$ and $\mathbf{W}$ and the beam selection functions $f_{\mathrm{T}}(\cdot)$ and $f_{\mathrm{R}}(\cdot)$. The Tx and Rx beam synthesizers have the same architecture.

D. Baselines and Metrics

The proposed method optimizes the GF beam synthesizers and the probing beams through DL, hence is referred to as the DL-GF method. It will be compared with five baselines: the DL-CB method, the exhaustive search, the genie with DFT codebooks, the DFT+EGC method, and MRT+maximum ratio combining (MRC).

- **DL-CB** The DL-CB method replaces the Tx and Rx beam synthesizers with two classifiers that predict the optimal beam indices in the BS and UE codebooks. It is an extension of our previous work [22] to the MIMO scenario. To improve its accuracy, the DL-CB method can sweep the top few candidate beam pairs predicted by the classifiers. In our experiment, the best beam pair is be selected after trying all combinations of the top-3 predicted Tx and Rx

beams.

- **Exhaustive search** The exhaustive search sweeps and measures all combinations of beam pairs in the BS and UE codebooks and selects the beam pair with the highest received signal power. Since the measurements are corrupted by noise, the beam pair selected by the exhaustive search may not be optimal.
- **Genie DFT** A genie always selects the optimal beam pair in the BS and UE codebooks. It is the same as the exhaustive search when the measurement noise power is zero.
- **DFT+EGC** Only the BS has a codebook in the DFT+EGC baseline. The BS exhaustively tries all beams in its codebook while the UE uses the corresponding EGC vector for each Tx beam. The best beam pair is selected assuming no measurement noise. It is expected to perform better than the genie DFT baseline due to the additional degree of freedom at the UE.
- **MRT+MRC** Neither the BS nor the UE uses a codebook. The BS uses the optimal MRT beam while the UE uses the MRC beam. The BF gain can be computed through an eigen-decomposition of $\mathbf{H}^H\mathbf{H}$. The MRT+MRC baseline is the theoretical upper bound under the unit-power constraint and cannot be achieved under the stricter unit-modulus constraint.

One important performance metric for beam alignment is the SNR achieved by the selected beams. We will compare the average SNR as well as the SNR distribution across different baselines. Secondly, new UEs need to satisfy a minimum SNR requirement so that they can be discovered during the IA process and connect to the BS. This is generally not a concern for CB approaches that adopt uniform codebooks, but may be problematic when the probing beams are site-specific and have severe coverage holes. Therefore, we will also investigate the misdetection probability of UEs, which is the probability that a UE achieves below-threshold SNR with the strongest probing beam pair, formally defined as

$$\text{misdetection probability} = \mathop{\mathbb{E}}_{\mathbf{H}\in\mathcal{H}}\left[\mathbb{1}_{\mathcal{H}_{\text{IA}}}(\mathbf{H})\right]. \tag{16}$$

The SNR threshold is chosen to be -5 dB [24].

IV. Dataset

Four scenarios from the public DeepMIMO dataset [25] are considered to capture a wide range of propagation environments, including indoor and outdoor environments, 28 GHz and 60 GHz carrier frequencies, as well as line-of-sight (LOS) and non-line-of-sight (NLOS) UEs. The channel realizations are computed through ray-tracing with a state-of-the-art commercial-grade

TABLE I: Simulation Parameters

BS Antenna	8×8 UPA
BS codebook size	$16 \times 16 = 256$
UE Antenna	4×4 UPA
UE codebook size	$8 \times 8 = 64$
Antenna element	Isotropic
Carrier Frequency	Outdoor LOS (O1): 28 GHz Indoor (I3): 60 GHz Outdoor NLOS (O1 blockage): 28 GHz
Bandwidth (B)	100 MHz
Transmit Power (P_T)	O1: 20 dBm I3, BS 1: 10 dBm I3, BS 2: 20 dBm O1 blockage: 35 dBm
Noise PSD	-173 dBm / Hz
UE orientation range	$z : Unif(-\pi, \pi)$ $y : Unif(-\frac{\pi}{2}, \frac{\pi}{2})$ $x : Unif(-\frac{\pi}{2}, \frac{\pi}{2})$

software [26], which is one of the most accurate ways of simulating mmWave channels once the environment topology is specified. The BS and UEs adopt UPAs with half-wavelength spacing. The simulation parameters are summarized in Table I for the four scenarios described below.

O1 Scenario. The O1 scenario captures an outdoor urban street environment with LOS UEs. An illustration of the scenario is shown in Fig. 2a. We select BS 3 and UEs from row #800 to row #1200 from the original dataset. The BS is placed on the street side and a total of 72,581 UEs are placed on a uniform grid on the street. The carrier frequency is 28 GHz.

I3 Scenarios. The I3 scenarios captures an indoor office environment with both LOS and NLOS UEs. An illustration of the environment is shown in Fig. 2b. There are two BSs in this scenario: BS 1 is placed on the inside wall of the conference room and BS 2 is placed on the opposite wall. A grid of LOS UEs is placed inside the conference room and a grid of NLOS UEs is placed in the corridor outside. There are a total of 118,959 UEs and the carrier frequency is 60 GHz. We consider two scenarios based on this environment, each with one of the two BSs activated.

O1 Blockage Scenario. The O1 blockage scenario is artificially created based on the O1 scenario with a metal screen placed in front of the BS and two reflectors placed on both ends of the street, as illustrated in Fig. 2c. The carrier frequency is 28 GHz and there a total of 497,931 UE positions. While it may not be representative of practical mmWave deployments, the extreme topology allows us to gain some intuition on the beam patterns learned in this environment.

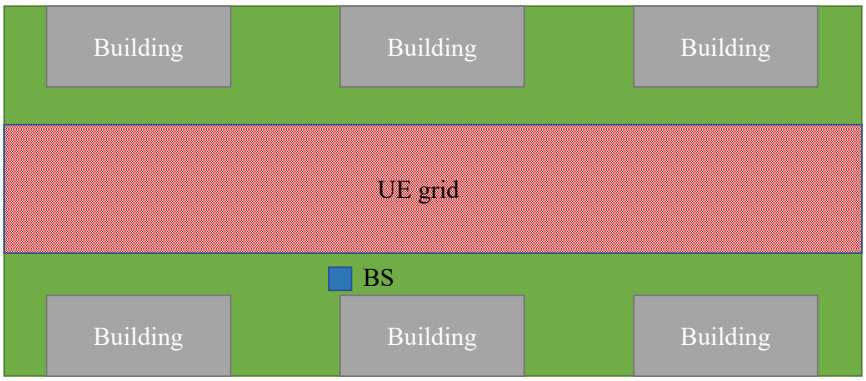

(a) O1

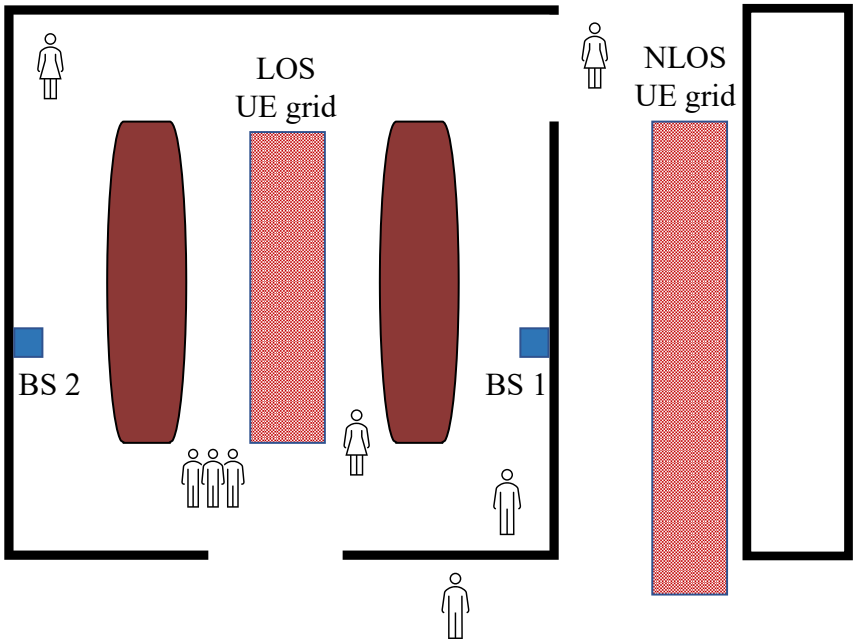

(b) I3

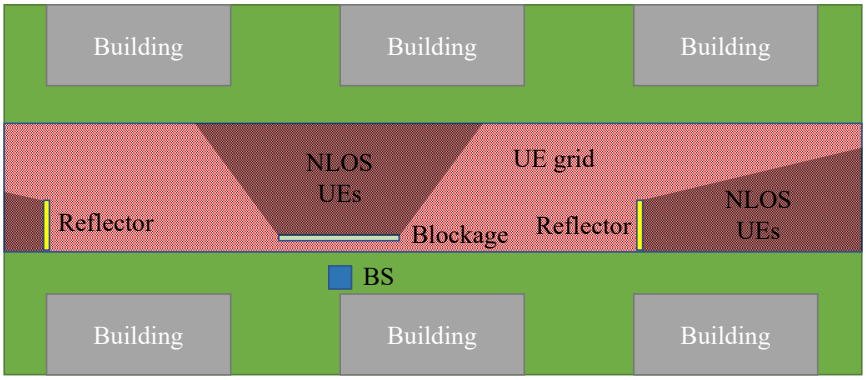

(c) O1 blockage

Fig. 2: Illustration of the DeepMIMO ray-tracing scenarios.

V. Evaluation

The datasets discussed in Section IV are partitioned so that 60% is used to train the NNs, 20% is used for validation and hyper-parameter tuning while we report the performance on the remaining 20% testing data. The NNs are trained for 4000 epochs with a batch size of 800 using the ADAM optimizer [27]. The γ parameter in the utility function is chosen to be 0.3 empirically. The measurement noise is AWGN. For CB baselines, the BS and the UE adopt over-sampled DFT codebooks with 256 and 64 beams respectively. The rest of the simulation parameters are summarized in Table I.

A. Gain of DL-GF vs. baselines

1) Can DL-GF Achieve Good SNR?: An ideal beam alignment method should quickly select near-optimal beams and achieve good SNR. The average SNR achieved by the proposed DL-GF method and the baselines in the more realistic O1 and I3 scenarios are shown in Fig. 3, 4, 5. It is evident that with the DL-CB approach, the beam classifiers can accurately select the best beam pairs. With increasing numbers of probing beam pairs, the average SNR achieved by the DL-CB baseline approaches that by the genie DFT. Nevertheless, its performance is limited by the resolution of the BS and UE codebooks since there is still a 1 dB gap between the DFT+EGC baseline and the genie DFT. On the other hand, the proposed DL-GF method improves upon DL-CB with its fully synthesized beams and is able to beat the exhaustive search with 20 probing beam pairs in the O1 scenario, 12 in I3 with BS 1 activated and 8 in I3 with BS 2 activated. It is eventually able to outperform the DFT+EGC baseline with as few as 20 probing beam pairs in the I3 scenarios and 32 in O1. A comparison of the 10th, 50th, 90th percentile and the average SNR with 32 probing beam pairs is shown in Table II. The proposed DL-GF method outperforms the exhaustive search everywhere in the distribution in both the O1 and the I3 scenario with BS 1 activated, and is only slightly worse in the 10th percentile SNR in the I3 scenario with BS 2 activated. Meanwhile, the misdetection probability is just 0.172%, 0.008% and 2.283% in the O1, I3 BS 1 and I3 BS 2 environments, guaranteeing that the vast majority of UEs can complete IA with one of the probing beams. The gain of DL-GF is twofold. First, in the probing phase, the site-specific probing beams allows the BS and the UE to capture crucial channel information with fewer measurements. Second, in the beam prediction phase, the beam synthesizer functions can be intuitively viewed as infinitely large codebooks, whose resolution in practice is only limited by the floating-point precision of the NN and the range of probing

TABLE II: SNR Comparison with 32 Probing Beam Pairs

Scenario	SNR (dB)	DL-GF	DL-CB top-3	Exhaustive search	Genie DFT	DFT+EGC	MRT+MRC
O1	10th %	11.229	10.571	10.630	10.835	11.744	12.421
	50th %	16.308	15.310	15.315	15.365	16.217	16.707
	90th %	20.558	19.689	19.713	19.723	20.517	20.918
	average	17.432	16.552	16.597	16.634	17.440	17.949
I3, BS 1	10th %	13.812	12.536	12.535	12.624	13.805	14.316
	50th %	16.519	15.354	15.353	15.385	16.269	16.771
	90th %	18.358	17.474	17.472	17.480	18.170	18.518
	average	16.620	15.541	15.542	15.572	16.402	16.879
I3, BS 2	10th %	5.508	5.536	5.793	6.185	7.246	8.090
	50th %	17.634	16.571	16.614	16.635	17.672	18.167
	90th %	23.391	22.351	22.351	22.358	23.131	23.529
	average	19.289	18.256	18.262	18.283	19.089	19.535

measurements. By generating analog beams at increased spatial resolutions that are also adapted to the specific environment, DL-GF achieves additional gain over the standard DFT codebooks.

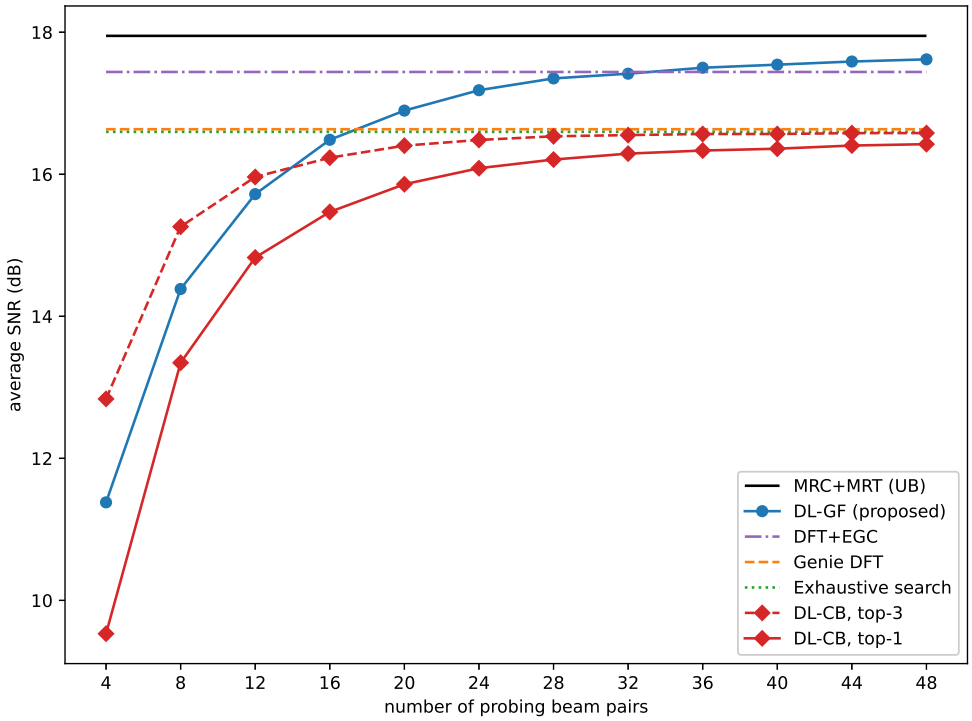

Fig. 3: The average SNR vs. number of probing beam pairs in the O1 scenario.

2) The SNR vs. Beam Alignment Speed Trade-off: Conventional CB beam alignment approaches can always find better beams more frequently by trying more candidates and increasing the resolution of the codebook. Similarly, the proposed DL-GF method can achieve better SNR

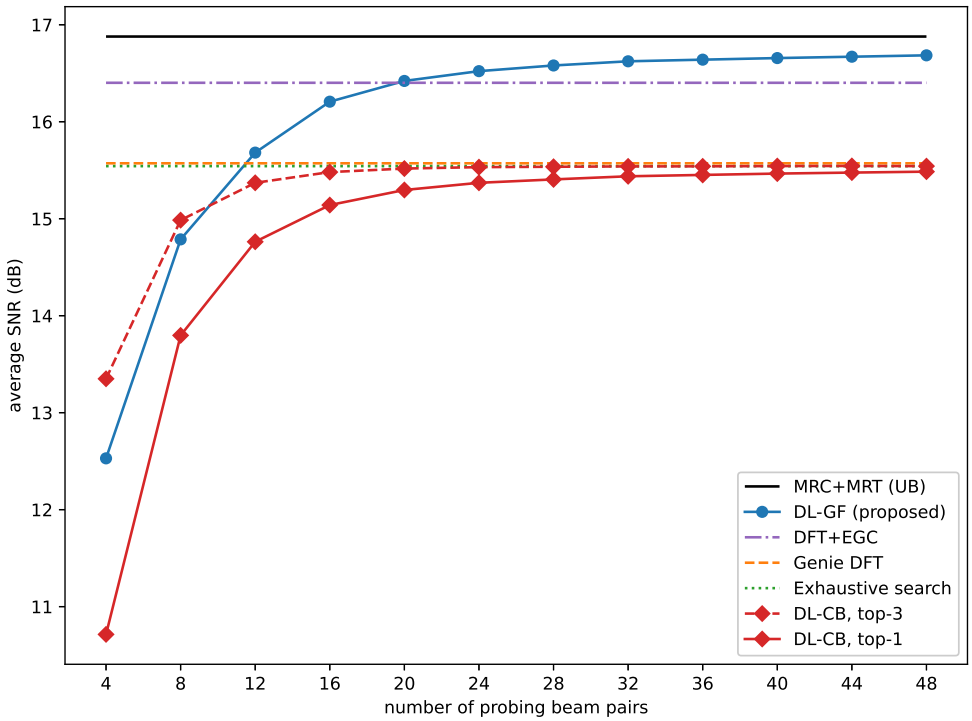

Fig. 4: The average SNR vs. number of probing beam pairs in the I3 BS 1 scenario.

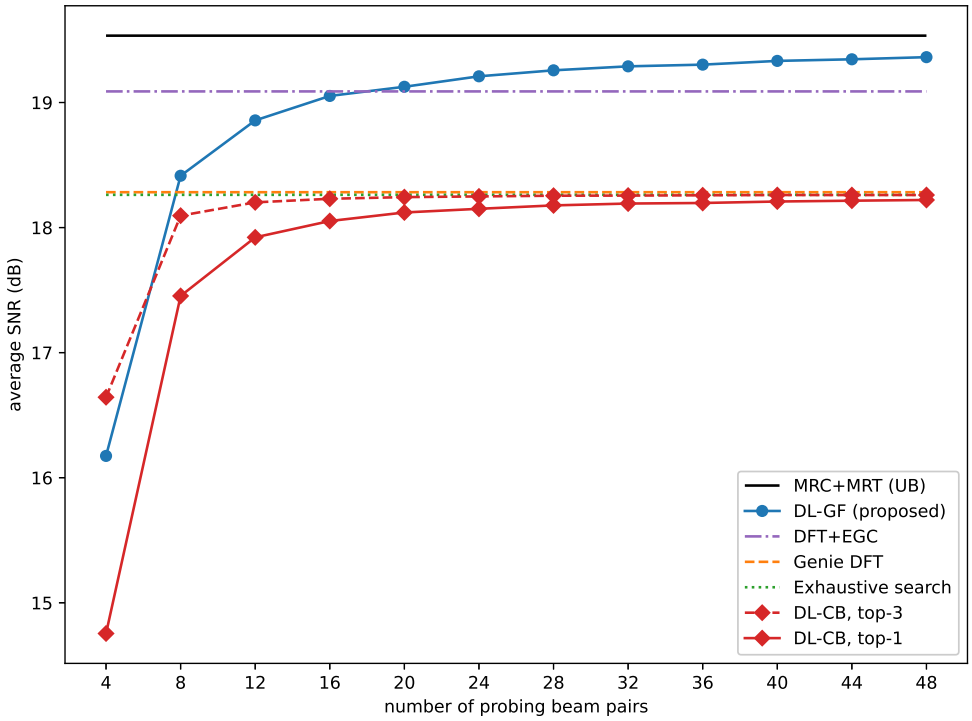

Fig. 5: The average SNR vs. number of probing beam pairs in the I3 BS 2 scenario.

by sweeping more probing beams. However, such SNR gain usually occurs at the cost of higher latency. In practical cellular systems with multiple UEs, the beam alignment procedure may need to be performed for each UE. It is therefore important for operators to consider the trade-off between the SNR and the overall beam alignment speed, which we define as the reciprocal of the total number of beams swept for all UEs. The average SNR achieved at each beam alignment speed for DL-GF, DL-CB and the exhaustive search is shown in Fig. 6. Compared to the exhaustive search, the proposed DL-GF method is better by 5 to 10 dB in terms of the average SNR at a given speed or faster by around two orders of magnitude when the achieved average SNR is from 10 to 15 dB. The proposed GF approach is also strictly better than the CB method, achieving 1-2.5 dB higher SNR at each beam alignment speed. With multiple UEs, other beam alignment methods that require an additional beam sweeping phase for each UE are expected to achieve a similar SNR-speed trade-off as the DL-CB with top-k search does. Since DL-GF is faster than DL-CB with top-3 search by an order of magnitude with 10 or 20 UEs, similar gains can be expected over methods such as the hierarchical search and active learning approaches. Interestingly, increasing the number of probing beams is often more efficient than searching more candidates for the DL-CB method, particularly when a high beam alignment speed is required.

A more detailed analysis of the total number of beams swept for different beam alignment methods in a cell with K UEs is shown in Table III. In the hierarchical search, the BS and the UE adopt 2-tier codebooks with $N_{\mathbf{F}}$ and $N_{\mathbf{W}}$ wide beams respectively. The BS first performs the Tx hierarchical search while the UE uses an omnidirectional Rx beam, then the UE performs the Rx hierarchical search. The exhaustive search requires sweeping all combinations of the M_{T} Tx beams and M_{R} Rx beams, which amounts to a total of 16,384 beam pairs in our setting. Methods such as the hierarchical search and DL-CB with top-k search require an additional beam sweeping phase for each UE. As a result, the overall beam sweeping overhead increases linearly with the number of UEs. On the other hand, since the proposed DL-GF method predicts the beams in one shot after sweeping a common set of probing beams for all UEs, its beam sweeping overhead is constant regardless of the number of UEs. In our setting, DL-GF reduces the beam sweeping overhead by over 500× while scaling optimally with increasing number of UEs.

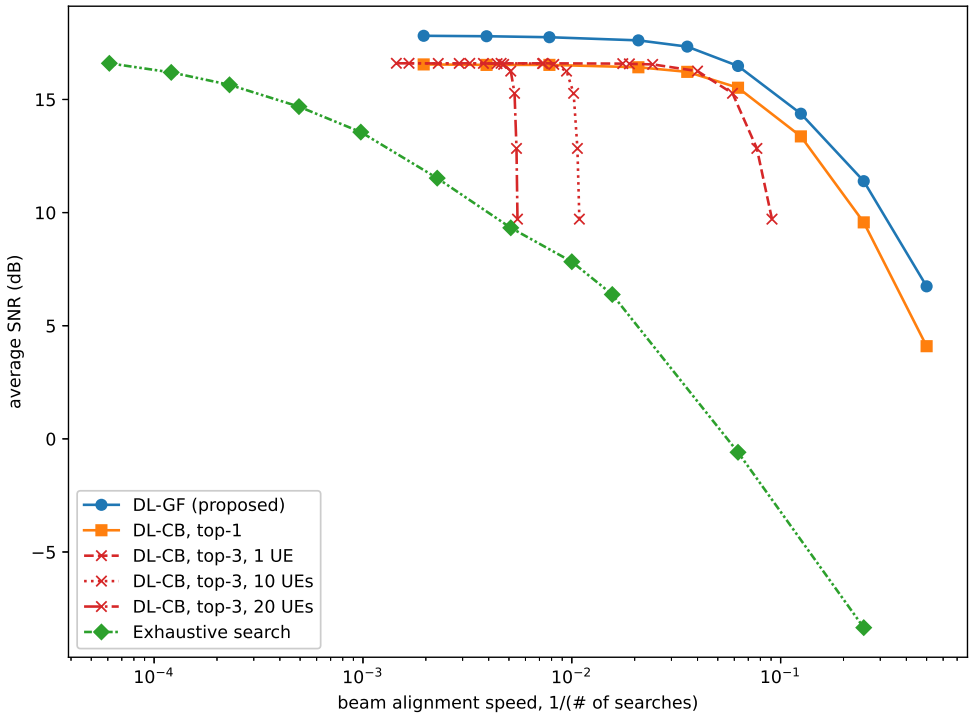

Fig. 6: Average SNR vs. the total beam alignment speed in the O1 scenario.

TABLE III: Beam Sweeping Overhead for K UEs

Beam alignment method	**Beam sweeping overhead**	**Feedback overhead**
DL-GF	N_{probe}	KN_{probe} power values
DL-CB, top-k	$N_{\text{probe}} + \min(K \cdot k_{\mathbb{1}_{\{k>1\}}}, M_{\text{T}}M_{\text{R}})$	KN_{probe} power values + $K \cdot \mathbb{1}_{\{k>1\}}$ beam indices
Hierarchical search with $N_{\mathbf{F}}, N_{\mathbf{W}}$ Tx and Rx wide beams	$N_{\mathbf{F}} + \min(K\frac{M_{\text{T}}}{N_{\mathbf{F}}}, M_{\text{T}}) + N_{\mathbf{W}} + \min(K\frac{M_{\text{R}}}{N_{\mathbf{W}}}, M_{\text{R}})$	$4K$ beam indices
Exhaustive search of $M_{\text{T}}, M_{\text{R}}$ Tx and Rx beams	$M_{\text{T}}M_{\text{R}}$	K beam indices

B. Intuition behind the learned beams

To better understand how the probing beam pairs and the beam synthesizer functions achieve better performance, we investigate the learned beam patterns in the O1 Blockage scenario. For easier visualization, the BS and the UEs are equipped with uniform linear array (ULA) arrays that only beamform in the azimuth domain. A UE located on the left of the BS is selected from the testing dataset as a case study. With 4 probing beam pairs, the Tx and Rx probing patterns are heavily adapted to the propagation environment by directing most of the energy towards the reflectors on both ends of the street while avoiding the blockage in the broadside direction, as

shown in Fig. 7. On the other hand, the synthesizers predict sub-optimal beams. Both the Tx and Rx beams have a main lobe pointing roughly towards the UE. The Rx beam has two strong lobes while the Tx beam has a single narrow main lobe. As the number of probing beam pairs is increased to 20, the learned probing beams have much larger spatial coverage, as shown in Fig. 8. This is particularly noticeable in the Rx probing beams since the range of AoA is much larger compared to that of the AoD with random UE orientations and more variations in the location of UEs. Utilizing the increased information gathered by the probing beams, the beam synthesizers also learn to focus energy more accurately and precisely. Both the predicted Tx and Rx beams are narrower, have a single lobe and point more accurately at the UE. Overall, this allows DL-GF to achieve better SNR by adopting more probing beams.

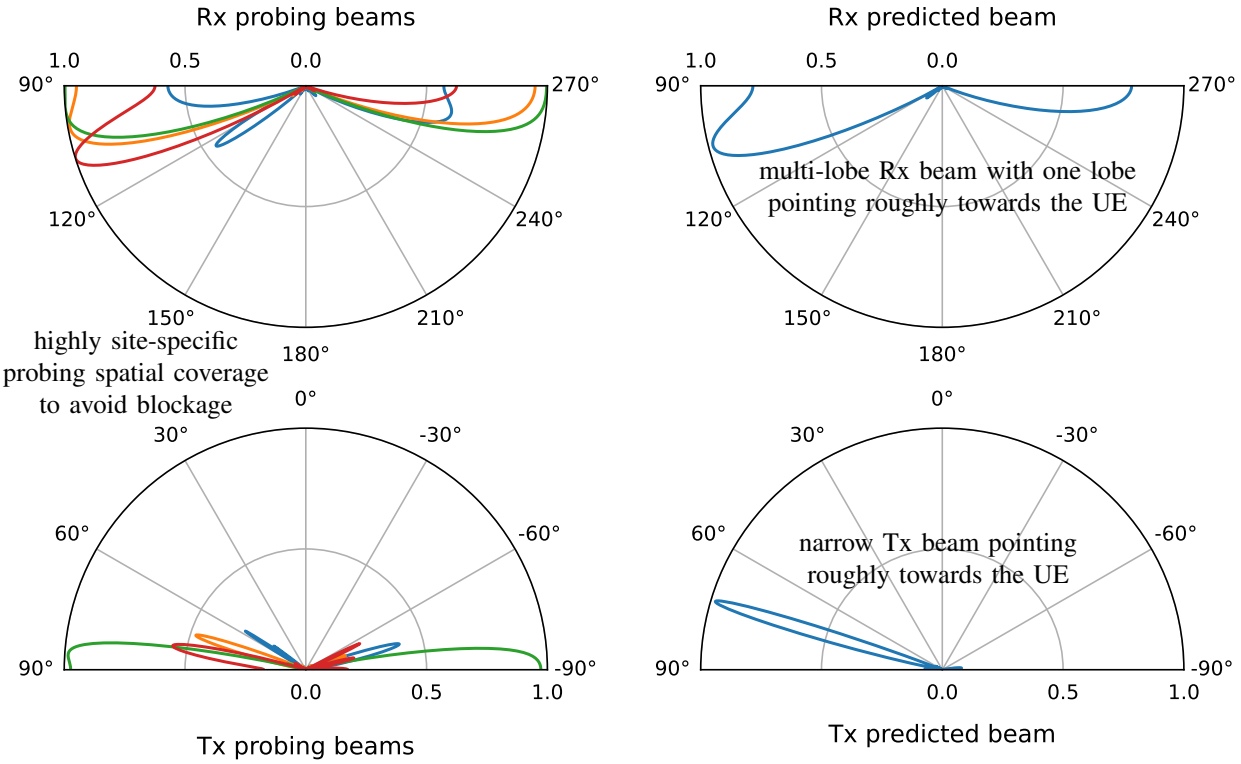

(a) Learned probing beam pairs

(b) Predicted beam pair for communication

Fig. 7: Radiation patterns of learned probing beam pairs and predicted beams in the O1 blockage scenario, $N_{\text{probe}} = 4$.

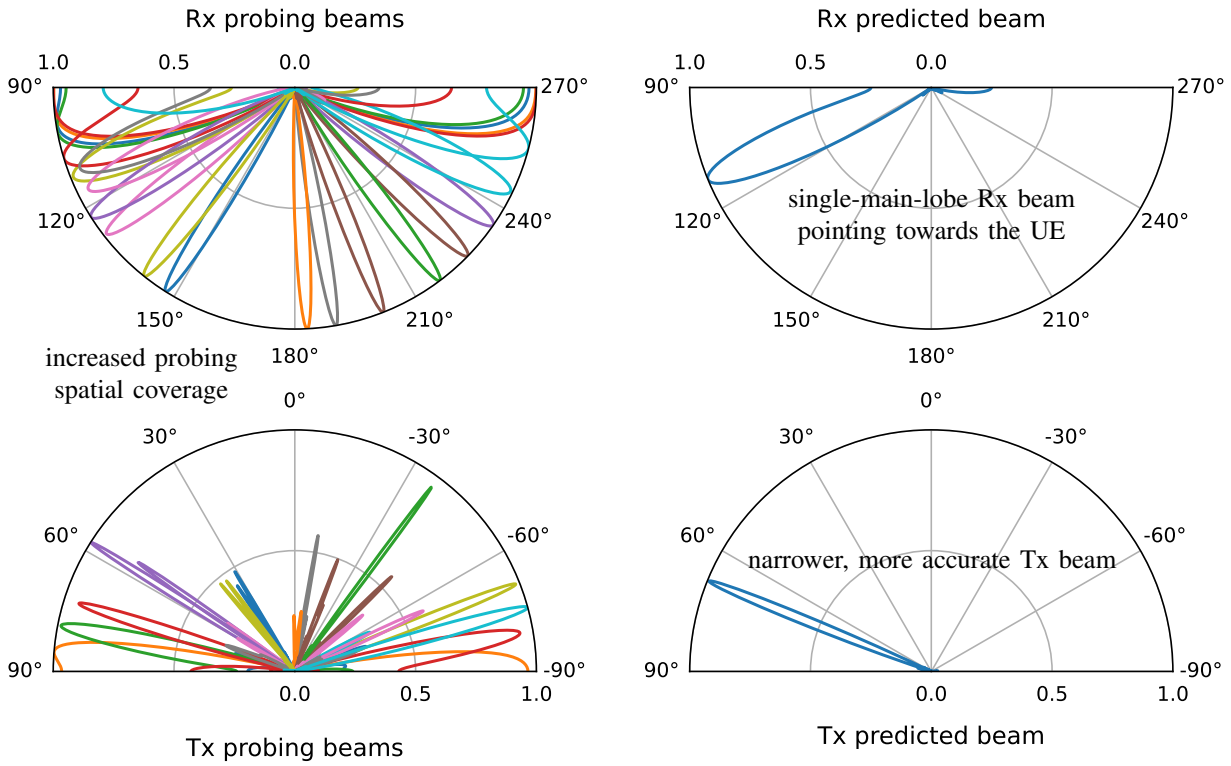

(a) Learned probing beam pairs

(b) Predicted beam pair for communication

Fig. 8: Radiation patterns of learned probing beam pairs and predicted beams in the O1 blockage scenario, $N_{\text{probe}} = 20$.

C. Robustness of DL-GF

1) Robustness to Noisy Measurements: The beam synthesizers rely on the probing measurements to generate the BF weights. While measurement noise can cause search errors in exhaustive and hierarchical searches, it can also impact the prediction of the NN models. A comparison of the average SNR with increasing measurement noise power spectral density (PSD) is shown in Fig. 9. As expected, the performance of the DL-GF, DL-CB and exhaustive search deteriorates with increasing measurement noise power, which becomes noticeable with noise PSD larger than -167 dBm/Hz. The exhaustive search is the most robust when the noise PSD is less than -143 dBm/Hz, while the one-shot DL-GF and DL-CB methods performs similarly. The DL-CB baseline is trained at each noise PSD level and can improve its robustness to noise by trying the top-3 candidates. There is also significant gain from training the DL-GF models at each noise

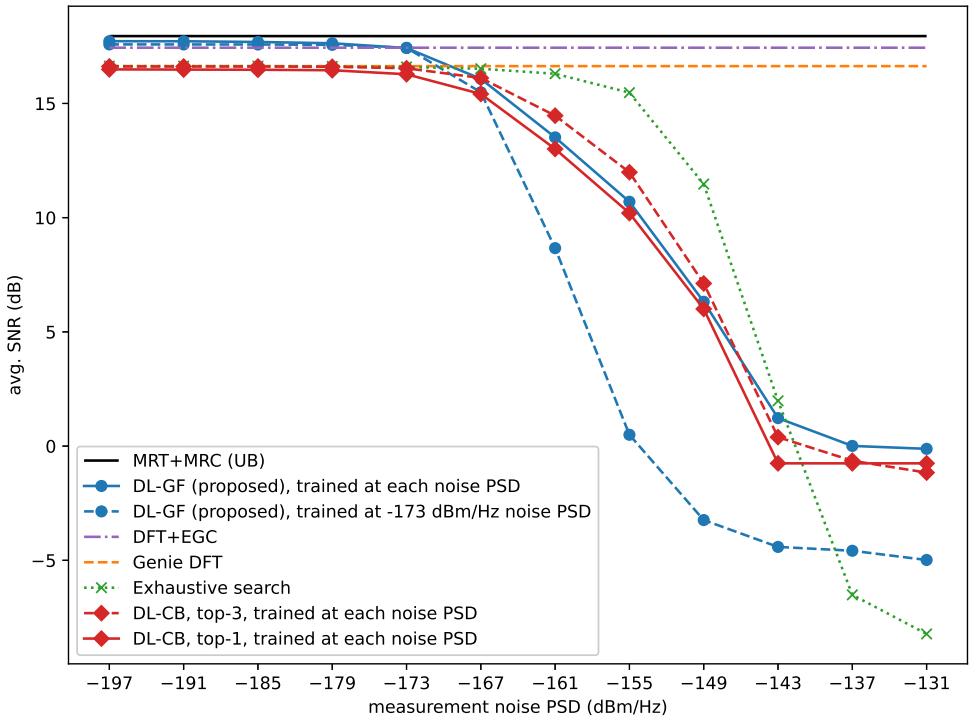

Fig. 9: Comparison of the average SNR with increasing measurement noise PSD in the O1 scenario. The DL-GF and DL-CB methods have 32 probing beam pairs.

PSD level compared to training with a fixed measurement noise power and testing with higher noise power. Interestingly, the average SNR of the exhaustive search becomes the worst when the measurement noise PSD reaches -137 dBm/Hz while that of the DL-based methods plateaus at around -143 dBm/Hz. At this point, the exhaustive search is essentially producing randomly guesses since the beam measurements are dominated by noise. On the other hand, the DL-based methods converge to always predict the same beam pair. In the case of DL-CB, the predicted beam pair happens to be the most frequent optimal beam pair.

2) Robustness to Imperfect Training Data: Training DL models typically requires high-quality data. While ray-tracing is one of the most accurate ways to simulate mmWave channels, it is not easily scalable to a city-wide deployment and the generated data may still differ from actual channels due to mismatched environments and imperfect propagation models. If the training data is acquired through measurement campaigns, noisy measurement and channel estimation errors would also affect the quality of the data. It is therefore important to investigate the performance of the proposed method when there is a mismatch between the channels used for

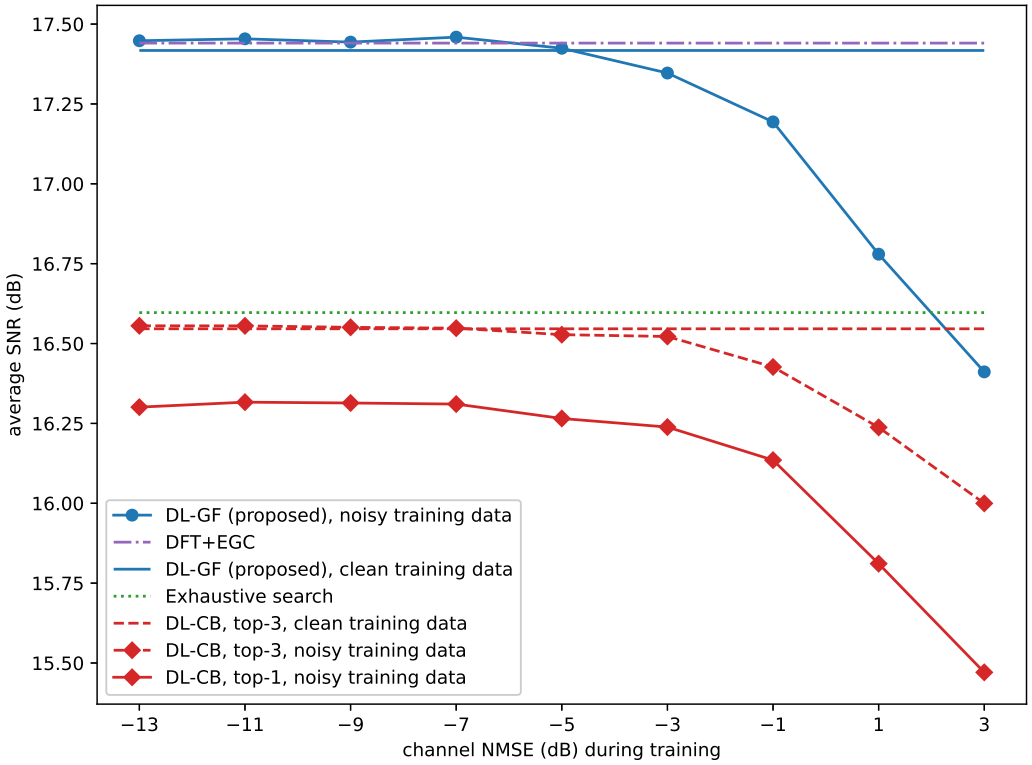

Fig. 10: Comparison of the average SNR with increasing training channel NMSE in the O1 scenario. The DL-GF and DL-CB methods have 32 probing beam pairs.

training and the actual channels during deployment. To simulate imperfect training data, the training channel matrices are corrupted with AWGN while the model is tested on clean channel data. The average SNR of the proposed DL-GF method, the DL-CB baseline and the exhaustive search with increasing normalized mean square error (NMSE) in the training data is shown in Fig. 10. Both the DL-GF and the DL-CB methods are relatively robust to noisy training data, experiencing little performance degradation when the channel NMSE is smaller than -3 dB. A small amount of noisy in the training data actually benefits the proposed DL-GF method, which is a common phenomenon in ML where noisy training data can sometimes improve the robustness and generalizability of ML models [28]. Even with a channel NMSE of 1 dB, the proposed DL-GF method can still outperform the exhaustive search and the DL-CB baseline trained on clean data. The added noise likely does not fundamentally shift the distribution of channels but instead makes it more “fuzzy”. During the unsupervised training procedure, the proposed NNs still learn to beamform on these noisy channels and generalize well to the clean actual channels.

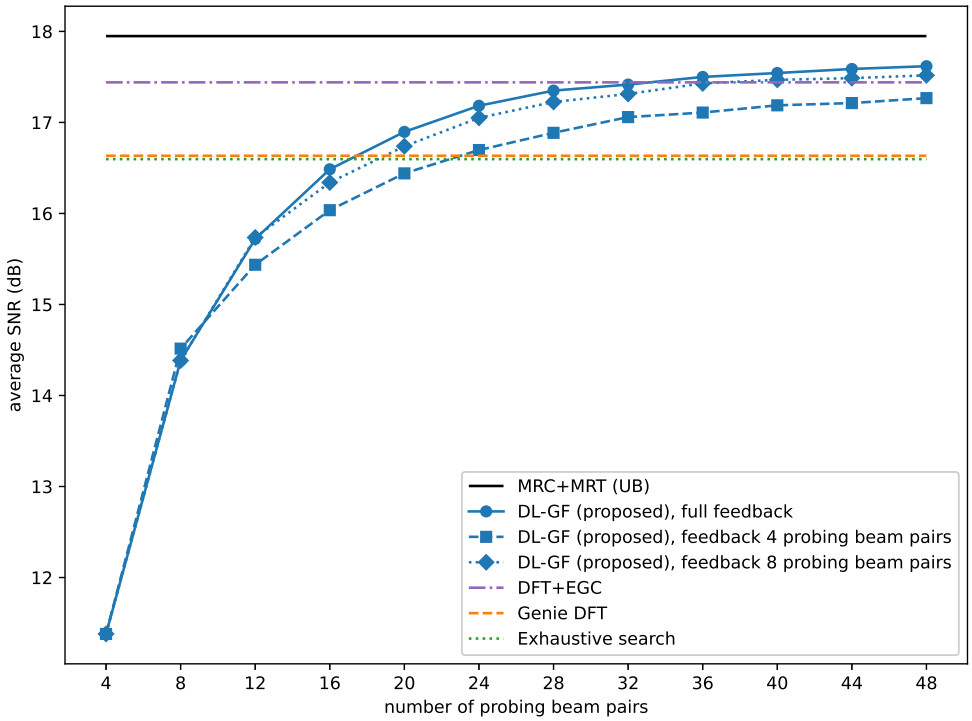

Fig. 11: Average SNR vs. the number of probing beam pairs with different feedback constraints.

3) Reducing the Feedback Overhead: The gain of DL-GF can be partially attributed to the much richer uplink feedback: it uses all the measurements as feature vectors to synthesize the BF weights instead of simply selecting the strongest beam. The feedback overhead of different methods are summarized in Table III. To reduce the feedback overhead, UEs can report measurements of a few strongest probing beam pairs. The vector $\mathbf{z}$ is masked so that only the top-m highest measurements are non-zero and the NN is trained from scratch. Since the shape of the feature vector is roughly maintained, reducing the feedback only results in a small degradation in the average SNR, as shown in Fig. 11. For instance, with 32 probing beam pairs in total, the average SNR drops by 0.4 dB when reporting 4 beam pairs and by only 0.12 dB when reporting the best 8. Note that f_{T} and f_{R} use the same masked feature vector in our experiments. In practice, the UE may use the full measurement vector to synthesize its beam while the BS uses the reduced feature, which will likely lead to even smaller performance loss.

4) Impact of Random UE Orientations: The orientation of UEs has a large impact on the performance of the proposed DL-GF method. A comparison of the average SNR and the misdetection probability with and without random UE rotation in the O1 scenario is shown in Fig. 12.

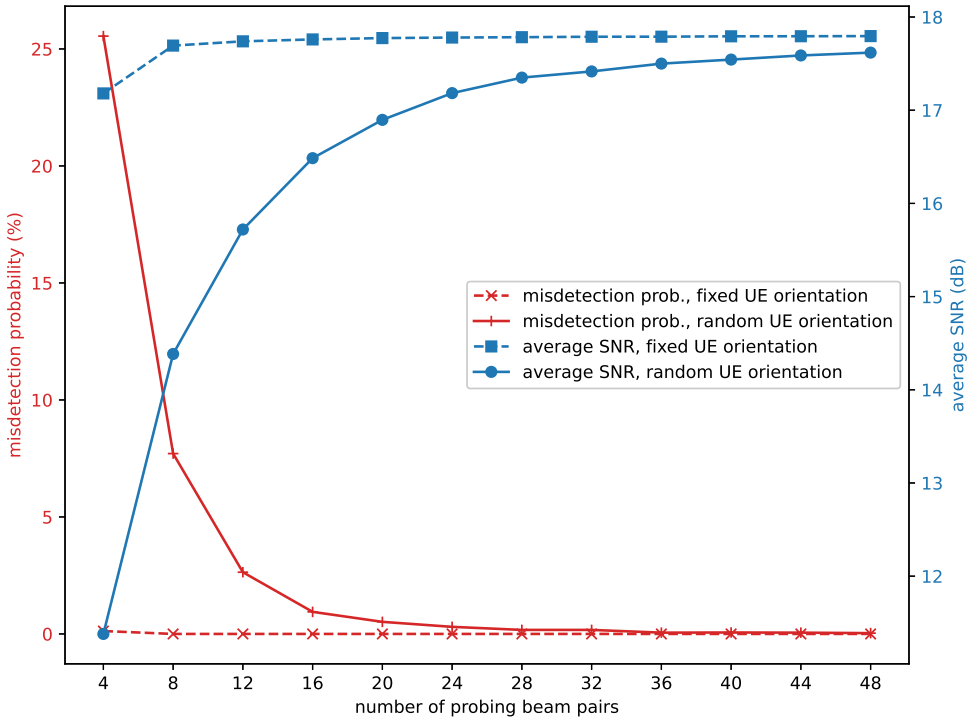

Fig. 12: The average SNR and misdetection probability of the proposed DL-GF method with and without random UE orientations in the O1 scenario.

Without random UE rotation, the proposed method can achieve better average SNR and lower misdetection probability with significantly fewer probing beam pairs. The random UE rotation increases the effective range of AoA. As a result, more probing beams are required to capture sufficient channel information on the UE side. The UE's probing beams also need to distribute energy and cover a larger angular space, leading to reduced BF gain and worse misdetection probability.

5) Reducing the Misdetection Probability: The ideal beam alignment solution should not only achieve high BF gain for connected UEs, but also be able to discover new UEs and allow them to complete IA. With the proposed DL-GF method, a new UE can do so with one of the probing beam pairs if it satisfies a minimum SNR requirement. Naturally, adopting more probing beams will allow each to cover a smaller angular space, thus increasing the gain of the probing beams and reducing the misdetection probability. By explicitly incorporating the IA performance in the utility function, we provide another tuning nob to reduce the misdetection probability. The proposed utility function can indeed further reduce the misdetection probability when the number

of probing beam pairs is fixed, as shown in Fig. 13a. Compared to simply optimizing the BF gain of the synthesized beams ($\gamma = 1.0$), incorporating the IA performance ($\gamma = 0.3$) reduces the misdetection probability by roughly 5 percentage points with 4 probing beam pairs and by 2 percentage points with 12 probing beam pairs while suffering from little SNR loss. Although the gain diminishes with more probing beams, the two-component utility function still provides a powerful tool to improve the IA coverage when the number of probing beams is limited. Since the $\mathcal{U}_{\text{IA}}$ term only covers UEs below a specified SNR threshold, the proposed utility function also allows the NN model to adapt to different SNR requirements for IA. As shown in Fig. 13b, the misdetection probability is reduced at various SNR threshold values for IA. The gain increases if a higher SNR threshold is adopted.

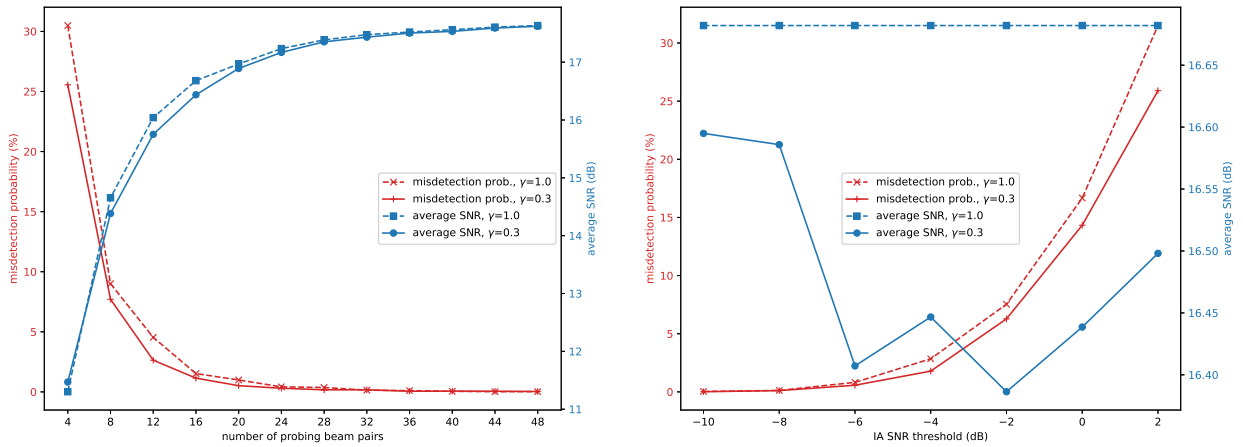

(a) vs. different numbers of probing beam pairs

(b) vs. different SNR threshold for IA

Fig. 13: The misdetection probability and average SNR with different γ in the O1 scenario.

VI. Conclusion

We propose a beam alignment method that directly synthesizes the analog beams in one shot after sweeping a few probing beam pairs and design a NN architecture to optimize the probing beams and beam synthesizer functions through site-specific training. Beating existing methods in terms of the overall SNR-speed trade-off often by orders of magnitude, the proposed method provides a promising new paradigm for mmWave beam alignment. Next-generation cellular systems can reap the benefits without overhauling the existing beam sweeping-based framework: the probing beams can be transmitted using periodic RSs while traditional beamforming codebooks

are replaced with NN beam synthesizers. Operators can select the number of probing beams based on the SNR and IA coverage requirement for each site.

There are many possible directions that this line of research could be extended, many of which have been identified throughout the paper. For example, scaling the site-specific training to city-wide networks and online adaptation to dynamic environments remain open research problems. The beam alignment problem has mostly been investigated to date from the BS point of view. It is important to also consider the unique beam alignment challenges on the UE side arising from multiple antenna panels, precarious dynamic rotations and more demanding power management.

REFERENCES

[1] Y. Heng and J. G. Andrews, "Grid-less mmWave beam alignment through deep learning," accepted at IEEE GLOBECOM 2022.

[2] M. Giordani, M. Polese, A. Roy, D. Castor, and M. Zorzi, "A tutorial on beam management for 3GPP NR at mmWave frequencies," *IEEE Commun. Surv. Tut.*, vol. 21, no. 1, pp. 173–196, Sep. 2019.

[3] Y. Heng, J. G. Andrews, J. Mo, V. Va, A. Ali, B. L. Ng, and J. C. Zhang, "Six key challenges for beam management in 5.5G and 6G systems," *IEEE Commun. Mag.*, vol. 59, no. 7, pp. 74–79, Jul. 2021.

[4] Z. Xiao, T. He, P. Xia, and X.-G. Xia, "Hierarchical codebook design for beamforming training in millimeter-wave communication," *IEEE Trans. Wireless Commun.*, vol. 15, no. 5, pp. 3380–3392, May 2016.

[5] C. Qi, K. Chen, O. A. Dobre, and G. Y. Li, "Hierarchical codebook-based multiuser beam training for millimeter wave massive MIMO," *IEEE Trans. Wireless Commun.*, vol. 19, no. 12, pp. 8142–8152, Sep. 2020.

[6] A. Ali, N. González-Prelcic, and R. W. Heath, "Millimeter wave beam-selection using out-of-band spatial information," *IEEE Trans. Wireless Commun.*, vol. 17, no. 2, pp. 1038–1052, Feb. 2018.

[7] Y. Heng and J. G. Andrews, "Machine learning-assisted beam alignment for mmWave systems," *IEEE Trans. Cogn. Commun. Netw.*, vol. 7, no. 4, pp. 1142–1155, May 2021.

[8] V. Va, J. Choi, T. Shimizu, G. Bansal, and R. W. Heath, "Inverse multipath fingerprinting for millimeter wave V2I beam alignment," *IEEE Trans. Veh. Technol.*, vol. 67, no. 5, pp. 4042–4058, Dec. 2017.

[9] N. González-Prelcic, R. Méndez-Rial, and R. W. Heath, "Radar aided beam alignment in mmWave V2I communications supporting antenna diversity," in *Proc. Inf. Theory and Appl. Workshop (ITA)*, Feb. 2016, pp. 1–5.

[10] U. Demirhan and A. Alkhateeb, "Radar aided 6G beam prediction: Deep learning algorithms and real-world demonstration," in *Proc. IEEE WCNC*, Apr. 2022, pp. 2655–2660.

[11] B. Salehihikouei, G. Reus-Muns, D. Roy, Z. Wang, T. Jian, J. Dy, S. Ioannidis, and K. Chowdhury, "Deep learning on multimodal sensor data at the wireless edge for vehicular network," *IEEE Trans. Veh. Technol.*, vol. 71, no. 7, pp. 7639–7655, Apr. 2022.

[12] W. Xu, F. Gao, S. Jin, and A. Alkhateeb, "3D scene-based beam selection for mmWave communications," *IEEE Wireless Commun. Letters*, vol. 9, no. 11, pp. 1850–1854, Jun. 2020.

[13] M. N. Khormuji and R.-A. Pitaval, "Statistical beam codebook design for mmWave massive MIMO systems," in *Proc. IEEE EuCNC*, Jun. 2017, pp. 1–5.

[14] W. Liu and Z. Wang, "Statistics-assisted beam training for mmWave massive MIMO systems," *IEEE Commun. Letters*, vol. 23, no. 8, pp. 1401–1404, Jun. 2019.

[15] M. Alrabeiah, Y. Zhang, and A. Alkhateeb, "Neural networks based beam codebooks: Learning mmWave massive MIMO beams that adapt to deployment and hardware," *IEEE Trans. Commun.*, vol. 70, no. 6, pp. 3818–3833, Apr. 2022.

[16] Y. Zhang, M. Alrabeiah, and A. Alkhateeb, "Reinforcement learning of beam codebooks in millimeter wave and terahertz MIMO systems," *IEEE Trans. Commun.*, vol. 70, no. 2, pp. 904–919, Nov. 2021.

[17] W. Ma, C. Qi, and G. Y. Li, "Machine learning for beam alignment in millimeter wave massive MIMO," *IEEE Wireless Commun. Letters*, vol. 9, no. 6, pp. 875–878, Jun. 2020.

[18] X. Li and A. Alkhateeb, "Deep learning for direct hybrid precoding in millimeter wave massive MIMO systems," in *Proc. IEEE Asilomar*, Nov. 2019, pp. 800–805.

[19] D. J. Love and R. W. Heath, "Equal gain transmission in multiple-input multiple-output wireless systems," *IEEE Trans. Commun.*, vol. 51, no. 7, pp. 1102–1110, Jul. 2003.

[20] K. M. Attiah, F. Sohrabi, and W. Yu, "Deep learning for channel sensing and hybrid precoding in TDD massive MIMO OFDM systems," *IEEE Trans. Wireless Commun.*, Jul. 2022, early access.

[21] F. Sohrabi, T. Jiang, W. Cui, and W. Yu, "Active sensing for communications by learning," *IEEE Journal on Sel. Areas in Communications*, vol. 40, no. 6, pp. 1780–1794, Mar. 2022.

[22] Y. Heng, J. Mo, and J. G. Andrews, "Learning site-specific probing beams for fast mmWave beam alignment," *IEEE Trans. Wireless Commun.*, vol. 21, no. 8, pp. 5785–5800, Jan. 2022.

[23] 3GPP, "Technical Specification Group Radio Access Network; Study on channel model for frequencies from 0.5 to 100 GHz," 3rd Generation Partnership Project (3GPP), Technical Report (TR) 38.901, Dec. 2019, version 16.1.0.

[24] M. Giordani, M. Mezzavilla, and M. Zorzi, "Initial access in 5G mmWave cellular networks," *IEEE Commun. Mag.*, vol. 54, pp. 40–47, Nov. 2016.

[25] A. Alkhateeb, "DeepMIMO: A generic deep learning dataset for millimeter wave and massive MIMO applications," in *Proc. Inf. Theory and Appl. Workshop (ITA)*, Feb. 2019, pp. 1–8.

[26] *Wireless InSite 3.2.0 Reference Manual*, Remcom Inc., 2017. [Online]. Available: https://www.remcom.com/wireless-insite-em-propagation-software/

[27] D. P. Kingma and J. Ba, "Adam: A method for stochastic optimization," in *Proc. ICLR*, 2015.

[28] I. Goodfellow, Y. Bengio, and A. Courville, *Deep Learning*. MIT Press, 2016, ch. 7, [Online.] Available: http://www.deeplearningbook.org.